GENERATION OF CONTINUOUS POLARIZATION DISTRIBUTION IN A SINGLE LASER BEAM

Ana BĂRAR[1], Octavian DĂNILĂ[2], Paul ŞCHIOPU[3]

We present a simple method to achieve continuously distributed elliptical polarization in a one-beam configuration, without the presence of interference effects in the detected beam. The construction relies on the polarization-to-spatial coordinate conversion of the beam, and can be tuned to compensate any optical path difference between the different polarization components in the beam. The method and any devices resulting from it may find extended applications in distributed communication systems that rely on polarization encoding rather than wavelength division multiplexing.

Keywords: polarization optics, anisotropic crystals, polarization-division multiplexing, applied optics

1. Introduction

With the steep rise in the volume of data to be transferred by means of wavelength based encoders [1, 2, 3], an alternative encoding system which relies on polarization was devised [4]. Originaly used for security purposes [5, 6], polarization encryption of data has been gaining a foothold in large-data communication schemes over recent years, triggered by notable breakthroughs in the volume of data it can handle [7, 8], and the efficiency of data transfer [9]. However, a major technological requirement to produce polarization division mutiplexing (PDM) is the ability to create as many polarization states as possible, while keeping the crosstalk to a minimum[10]. To achieve this, the go-to device is the spatial light modulator (SLM) [11], which can create a discrete set of polarization states, by actively modifying the phase for each wavelength. Due to their physical structure, however, liquid crystals are extremely sensitive to any mechanical vibrations, and they present an inherent rotational momentum under the effects of external electric and magnetic fields [12, 13, 14, 15]. Depending on the variation of such fields, liquid crystal composites may also exhibit nonlinearities [16, 17, 18]. Under higher control fields, the long-term health of SLM-s is endangered, and its controlling stability starts to deteriorate at some time before the SLM is destroyed.

In this paper, we present a simple method to achieve a continuous elliptical polarization distribution, extending from a horizontal state, while avoiding interference-induced beam profile aberrations. The method consists of passing a divergent laser beam through a birefringent medium, thus creating a well-known continuous distribution of polarization across the beam profile. We characterize the resolution of the output beam and determine

[1]Ph. D. Student, Faculty of Electronics, Telecommunications and Information Technology, University "Politehnica" of Bucharest, Romania

[2]Lecturer, Faculty of Applied Sciences, University "Politehnica" of Bucharest, Romania, corresponding author: octavian.danila@physics.pub.ro

[3]Professor, Faculty of Electronics, Telecommunications and Information Technology, University "Politehnica" of Bucharest, Romania

the cross-talk threshold for the distribution. Moreover, we propose a simple optical path compensation method, in order to provide an informationally-secure signal. The method can be achieved with off-the-shelf parts, and provides a wide stability range in terms of incident divergence angles. Also, the resolution of the beam sampling system can be improved by having a high-precision translation stage for the polarization analyzer available.

2. **Theoretical background and model description**

It is well known that the polarization of light at the output of an anisotropic medium is determined by the optical properties of the medium along the optical axis set. Due to their periodic structure, optical crystals are usually the go-to anisotropic medium. For such crystals, the refractive indexes along the optical axis are linked by the well known relation:

$$\frac{x^2}{n_x^2}+\frac{y^2}{n_y^2}+\frac{z^2}{n_z^2}=1 \tag{1}$$

which constitutes the refractive index ellipsoid model. For an arbitrary direction given by an angle θ with respect to the axis (i.e. Oz), the refractive indexes are given by the ellpise that sections the ellipsoid and which has the respective propagation direction as a director. In the case of uniaxial crystals, two of the three refractive indexes become equal, and the above relation becomes [19]:

$$\frac{\cos^2\theta}{n_o^2}+\frac{\sin^2\theta}{n_e^2}=\frac{1}{n_{eff}^2(\theta)} \tag{2}$$

where $n_{eff}(\theta)$ is the effective refractive index experienced by the extraordinary mode along an arbitrary direction which is rotated by angle θ from the optical axis, $n_o = n_x = n_y$ is the ordinary refractive index, and $n_e = n_z$ is the extraordinary refractive index. In such systems, when changing the direction of propagation from the principal axis of the crystal to another direction, the polarization parallel to the axis of rotation of the secant ellipses will always experience a constant ordinary refractive index n_o. This axis is known as *the fast axis* - (f), due to the fact that the waves having the polarization parallel to it will always propagate the fastest. The axis perpendicular to the fast axis is known as *the slow axis* - (s), having $n_{eff}(\theta)$ as an associated refractive index. The revolution ellipsoid is presented in Figure 1. It can be seen that, on the slow axis the refractive index varies from n_o for a polarization which is parallel to the ordinary direction to n_e for a polarization which is parallel to the extraordinary one. During propagation, the two polarization components acquire an optical path difference, which results in a conversion from a linear to an elliptic state of polarization (SOP). The ellipticity of the state depends both on the refractive indexes n_o and $n_{eff}(\theta)$ on one hand, and the length of the crystal through which it travels on the other.

The proposed method to achieve continuous polarization distribution across the laser beam is to pass a spatially divergent laser beam through a birefringent medium, in such a way that the ouptput beam has a well defined polarization-to-coordinate relation. In our setup, the chosen medium was a single-order half-wave plate with the optical axis parallel to the input polarization of the non-divergent beam. This implies that for the normally-incident beam, there is no delay between the waves propagating on the fast and slow axes. However, when a divergent beam is incident on the wave plate, the non-normal components of the beam will experience different refractive indexes on the slow and fast

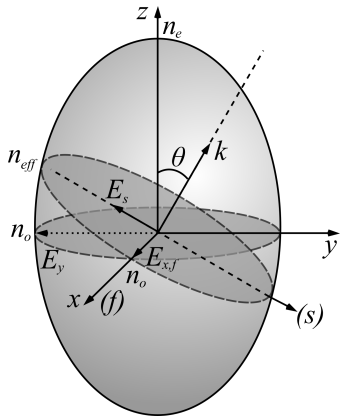

FIGURE 1. Illustration of the refractive index ellipsoid for a uniaxial crystal, depicting the refractive indexes experienced on an arbitrary direction, and the polarization components on the fast *(f)* and slow *(s)* axis set.

axes, together with a different optical length traveled in the medium. The propagation of the divergent beam through the uniaxial crystal is presented in Figure 2.

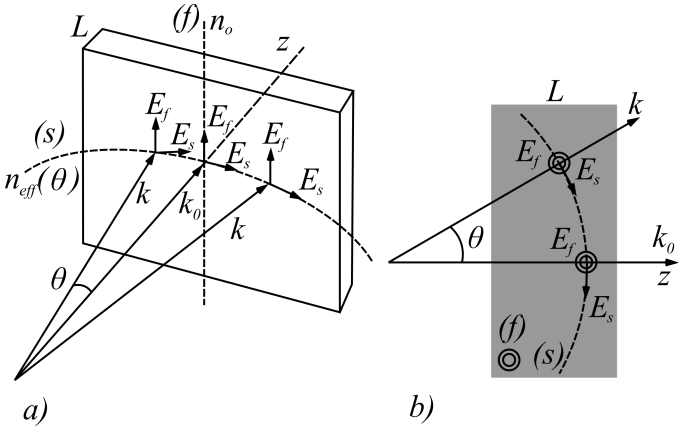

FIGURE 2. b) Illustration of the proposed working model: a) - the propagation of a divergent beam through a birefringent medium of a thickness L, the experienced refractive indexes and the polarization components on the fast and slow axes. b) - Top view of the divergent beam propagation through the uniaxial medium, highlighting the polarization states on the fast and slow axis, and the effective length traveled through the crystal by each part of the wave front

At the output of the wave plate, the divergent beam is re-collimated and a spatial scan of the profile is performed. To determine the relation that links the ellipticity of the SOP and the divergence angle via the optical properties of the medium, we consider a single-order wave plate of a given thickness L, for a beam propagating along a direction given by input angle θ. For this direction, the field vectors on the fast - *(f)* and slow - *(s)* axes of the at the output of the wave plate are:

$$E_f = A_f \cos\left(\omega\left(t - \frac{L}{c} n_o\right)\right) = A_f \cos\phi_f \tag{3}$$

for the ordinary ray, and:

$$E_s = A_s \cos\left(\omega\left(t - \frac{L}{c} n_{eff}(\theta)\right)\right) = A_s \cos\phi_s \tag{4}$$

where subscripts s and f denote the slow-fast axis set, and L is the effective length traveled in the wave plate, which for the single order wave plate is given as:

$$L = \frac{\lambda}{\cos\theta} \tag{5}$$

Also, the induced phase difference between the two propagating waves is $\phi = \phi_s - \phi_f$, which is strongly dependent on the direction angle through the effective refractive index $n_{eff}(\theta)$ and the effective optical length $L(\theta)$. Depending on the accumulated phase difference, the expression of the electric field describing the SOP is [20]:

$$\frac{E_f^2}{A_f^2} + \frac{E_s^2}{A_s^2} - 2\frac{E_f E_s}{A_f A_s}\cos\phi = \sin^2\phi \tag{6}$$

where $\phi(\theta)$ represents the induced phase difference for a wave propagating in the anisotropic medium. Assuming that the two components are in-phase at the input and due to the fact that the frequency of the wave does not change in material media, the accumulated phase difference is only induced by the optical path difference given by the different refractive indices. A general elliptical SOP can be characterized by the semiaxes A_f, A_s, by the azimuth angle[20]:

$$\tan\psi = \frac{2\tan\phi}{1-\tan^2\phi}\cos\phi \tag{7}$$

and by the ellipticity angle:

$$\sin 2\chi = \frac{2\tan\phi}{1-\tan^2\phi}\sin\phi \tag{8}$$

These parameters can be conveniently set as to generate the associated Stokes parameters of the SOP:

$$s_0 = A_f^2 + A_s^2; \quad s_1 = A_f^2 - A_s^2; \tag{9}$$

$$s_2 = 2A_f A_s \cos\phi; \quad s_3 = 2A_f^2 A_s^2 \sin\phi \tag{10}$$

From the above relations it can be deduced that $s_0^2 = s_1^2 + s_2^2 + s_3^2$. Moreover, the Stokes parameters can be expressed as a function of the ψ and χ angles as[19]:

$$s_1 = s_0 \cos 2\chi \cos 2\psi \tag{11}$$

$$s_2 = s_0 \cos 2\chi \cos 2\psi \tag{12}$$

$$s_3 = s_0 \sin 2\chi \tag{13}$$

Based on the above parametrization, it can be seen that the Stokes parameters are the components of a spherical representation vector system - the Poincaré sphere. The sphere is the basis of representation of any possible SOP in the *Oxyz* reference frame, with added information regarding the intensity, which is contained in s_0. Conversely, given a certain SOP, all information on the state can be given by measuring the Stokes vector components on each Cartesian axis.

3. **Device description and results**

The measurement setup is presented in Figure 3, and consists of the following: A continuous-wave (CW) laser source operating at 633 nm (Coherent He-Ne series), equipped with a Faraday isolator (EoTech Tornos series), emits a beam inside a modified mirror-based beam expander, having a half wave plate inside. The mirrors are identical, and the distance between them is calculated as to compensate for the divergence induced by the wave plate.

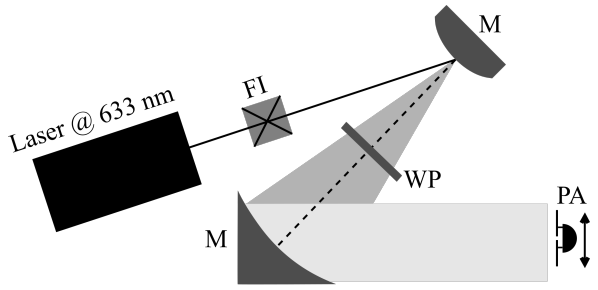

FIGURE 3. Illustration of the setup used to create the polarization distribution: FI - Faraday isolator, M - spherical mirror, WP - half wave plate, PA - polarization analyzer. The beam coming from the laser is spatially diverged by a convex mirror onto a half wave plate, to create the polarization distribution. The divergent beam is re-collimated by a convex mirror, in order to provide a linear one-dimensional scanning possibility.

Typically, when propagating along the optical axis, the polarization plane is rotated by introducing a phase delay between the ordinary and extraordinary axes. When the beam passes through the wave plate, at a given angle with respect to the optical axis, the different refractive indexes experienced on the ordinary and extraordinary directions, together with a different travel length in the medium cause the appearance of a certain ellipticity in the polarization state. By choosing mirrors with small radii in the beam expander, divergence angles of up to 60° can be established on the wave plate. Due to the spatial expansion, there is also a conversion between the coordinate of the beam on the input face of the plate and the incidence angle, with the center of the beam being ideally the normal incidence coordinate. The diameter of the output beam is given by the distance between the expander mirrors, as well as their radii of curvature. To evaluate the state of polarization (SOP), a polarization analyzer (Thorlabs PAX 1000 series) was used to scan the spatial profile of the beam along one dimension. The recorded position was converted to the divergence angle using the relation between the curvature radii of the mirrors and the distance between them.

To achieve high resolution scanning, the polarization analyzer was fitted with a spatial filter, with an opening of the size of hundreds of microns. Due to the symmetry of the angular distribution, the measurements were performed starting from the center of the beam, which corresponds to normal incidence, and up to the outer ring, on a given direction (either horizontal or vertical. Based on the beam diameter and the distances between the mirrors, the divergence angle of the beam on the wave plate was measured. To describe the SOP, Stokes parameters [19] measurements were performed. For ease of reading the

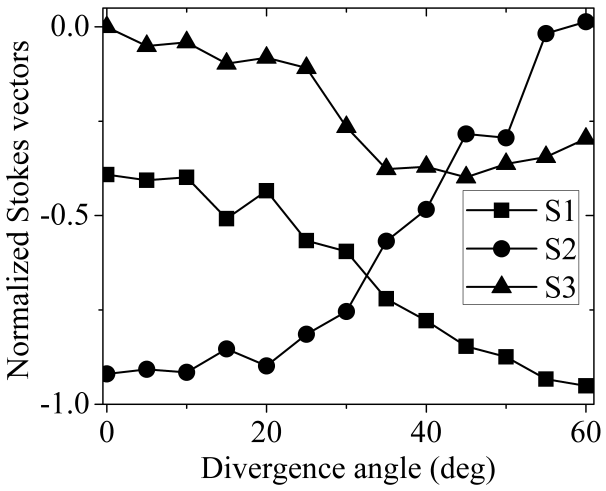

FIGURE 4. The normalized Stokes parameters that describe the SOP as a function of the calculated divergence angle of the beam hitting the wave-plate (the solid lines serve as guidelines for the eye).

normalized Stokes parameters s_k/s_0 were extracted and the results are presented in Figure 4.

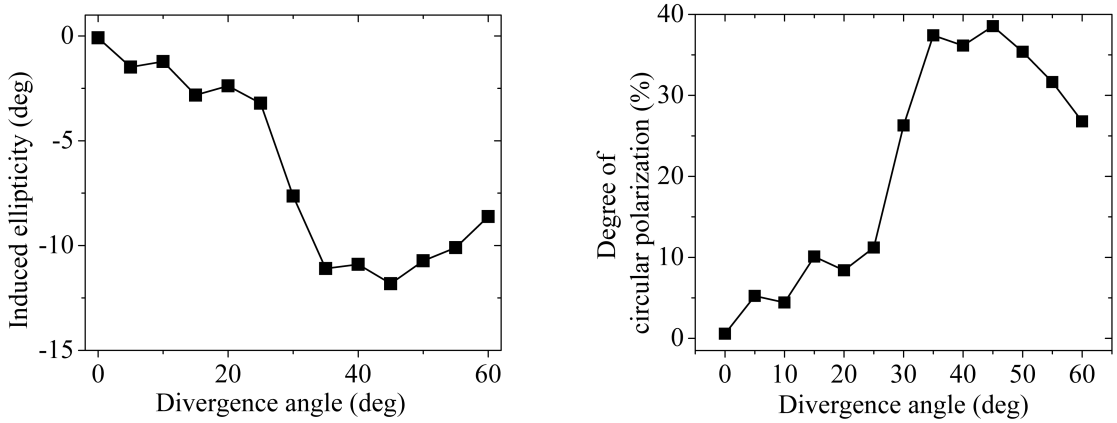

FIGURE 5. Left: The induced ellipticity angle as a function of the input divergence angle; Right: The induced degree of circular polarization in the SOP as a function of the input divergence angle (the solid lines serve as guidelines for the eye).

Separately, a measurement regarding the ellipticity angle of the SOP was performed, which was used to determine the degree of circular polarization induced by the divergence angle. The degree of circular polarization is given by the ratio:

$$DOCP = \frac{I_0 - I_{cp}}{I_0 + I_{cp}} \tag{14}$$

where I_0 is the full intensity of the beam, and I_{cp} is the intensity of the circularly polarized beam. The results are presented in Figure 5.

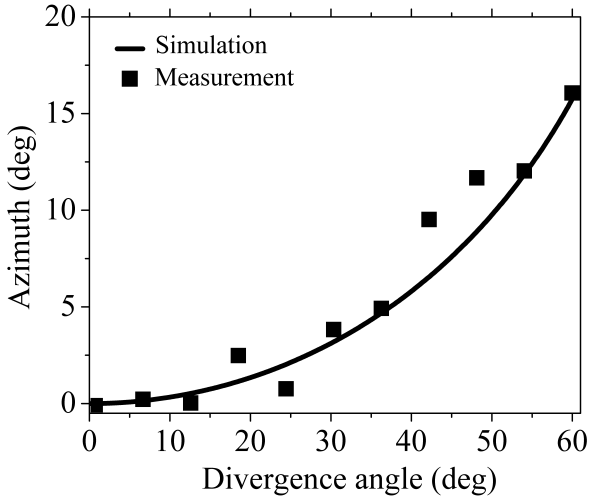

FIGURE 6. The azimuth of the linear polarization plane as a function of the input divergence angle.

Aside from the induced circular polarization, we performed measurements of the azimuth of the SOP with respect to the divergence angle. The azimuth of the linear polarization plane versus the divergence angle θ was theoretically determined using relation (7), and it was experimentally obtained for a single order quartz wave plate. The results are presented in Figure 6.

4. **Conclusions**

In this paper, we report the design of a method to generate a continuously-distributed elliptical polarization state throughout the spatial profile of a single laser beam. Apart from the standard SOP characterization, measurements regarding the variation of the linear polarization plane with respect to the divergence angle were performed. The distribution exhibits a good azimuthal stability for angles below 60°. The elliptical SOP is not monotonous throughout the whole angular interval, exhibiting a maximum at around 45°. This represents a boundary for the operation limit of the method.

REFERENCES

[1] S. Gunn. Optical fibre wavelength division multiplexing. In *Comsig88 Southern African Conference on Communication and Signal Processing, Pretoria, South Africa*, 1988.

[2] J. Z. Zhang, A. B. Wang, J. F. Wang, and Y. C. Wang. Wavelength division multiplexing of chaotic secure and fiber-optic communications. *Optics Express*, 8:6357–6367, 2009.

[3] A. Shahpari, R. Ferreira, V. Ribeiro, A. Sousa, Z. Somayeh, A. Tavares, Z. Vujicic, F. Guiomar, J. D. Reis, A. N. Pinto, and A. Teixeira. Coherent ultra dense wavelength division multiplexing passive optical networks. *Optical Fiber Technology*, 26:100–107, 2015.

[4] X. Tan, O. Matoba, Y. Okada-Shudo, M. Ide, T. Shimura, and K. Kuroda. Secure optical memory system with polarization encryption. *Applied Optics*, 40:2310–2315, 2001.

[5] O. Matoba and B. Javidi. Polarization encoding for optical security systems. *Optical Engineering*, 39:2439–2443, 2004.

[6] W. Chen, B. Javidi, and X. Chen. Advances in optical security systems. *Advances in Optics and Photonics*, 6:120–155, 155.

[7] M. A. Elmagzoub, A. B. Mohammad, R. Q. Shaddad, and S. A. Al-Gailani. Polarization multiplexing of two mimo rof signals and one baseband signal over a single wavelength. *Optics and Laser Technology*, 76:70–78, 2016.

[8] Z. Y. Chen, L. S. Yan, Y. Pan, L. Jiang, A. L. Yi, W. Pan, and B. Luo. Use of polarization freedom beyond polarization-division multiplexing to support high-speed and spectral-efficient data transmission. *Light: Science and Applications*, 6:e16207, 2017.

[9] J. W. Gossens, M. I. Yousefi, Y. Jaouën, and H. Hafermann. Polarization-division multiplexing based on the nonlinear fourier transform. *Optics Express*, 25:26439, 2017.

[10] R. Noé, S. Hinz, D. Sandel, and Wüst. Crosstalk detection schemes for polarization division multiplex transmission. *IEEE Journal of Lightwave Technology*, 19:1469–1475, 2001.

[11] M. Sugiyama T. Hara and M. Suzuki. A spatial light modulator. *Adv. Electron. Electron Phys.*, 64:637–647, 1985.

[12] C. Roşu, D. Mănăilă-Maximean, S Kundu, P. L. Almeida, and O. Dănilă. Perspectives on the electrically induced properties of electrospun cellulose/liquid crystal devices. *J. Electrostat.*, 69, 2011.

[13] E. Petrescu, C. Cîrtoaje, and O. Dănilă. Dynamic behavior of nematic liquid crystal mixtures with quantum dots in electric fields. *Beilstein Journal of Nanotechnology*, pages 399–406, 2018.

[14] D. Mănăilă-Maximean, C. Cîrtoaje, O. Dănilă, and D. Donescu. Novel colloidal system: Magnetite-polymer particles/lyotropic liquid crystal under magnetic field. *Journal of Magnetism and Magnetic Materials*, 438:132–137, 2017.

[15] D. Mănăilă-Maximean. New grafted ferrite particles/liquid crystal composite under magnetic field. *Journal of Magnetism and Magnetic Materials*, 452:343–348, 2018.

[16] C. Cîrtoaje, E. Petrescu, and C. Moţoc. Self-focusing in nematic liquid crystals subjected to magnetic fields. *Journal of Optoelectronics and Advanced Materials - Rapid Communications*, 5:106–111, 2011.

[17] V. Stoian, C. Cîrtoaje, E. Petrescu, and C. Moţoc. Nonlinearities induced by magnetic fields in nematic liquid crystals. *Optics Communications*, 309:286–290, 2013.

[18] V. Stoian, C. Cîrtoaje, E. Petrescu, and C. Moţoc. Optical nonlinearities induced by electric fields in nematic liquid crystals. *Proceedings of SPIE*, 9503, 2015.

[19] B. E. A. Saleh and M. C. Teich. *Fundamentals of Photonics*. John Wiley and Sons, Inc, 2001.

[20] M. Born and E. Wolf. *Principles of Optics*. Cambridge University Press, 1999.